TECHNICAL TRANSACTIONS | **CZASOPISMO TECHNICZNE**
CHEMISTRY | CHEMIA
2-Ch/2014

KRZYSZTOF WOJTAS*, ŁUKASZ MAKOWSKI*, WOJCIECH ORCIUCH*

MODELLING AND EXPERIMANTAL VALIDATION OF FLUID VELOCITY AND TRACER CONCENTRATION IN JET REACTORS

MODELOWANIE I WERYFIKACJA DOŚWIADCZALNA PÓL PRĘDKOŚCI I STĘŻENIA TRASERA W REAKTORACH ZDERZENIOWYCH

A b s t r a c t

The paper presents a collection of experimental data from particle image velocimetry and planar laser induced fluorescence methods containing local microstructures of fluid velocity and inert tracer concentration in jet reactors. The results of experiments, performed with resolution of the level of several microns, can be used for direct validation of CFD models, especially for time-dependent mixing model used in large eddy simulations.

Keywords: *jet reactors*, *mixing*, *piv*, *plif*, *les*

S t r e s z c z e n i e

W artykule przedstawiono wyniki badań doświadczalnych przeprowadzonych z wykorzystaniem zaawansowanych technik laserowych, takich jak anemometria laserowa i laserowo indukowana fluorescencja w celu uzyskania informacji na temat pola prędkości i stężenia trasera w wybranych typach reaktorów zderzeniowych. Wyniki eksperymentalne posłużyły do weryfikacji obliczeń numerycznych z wykorzystaniem obliczeniowej mechaniki płynów w szczególności modeli wielkowirowych.

Słowa kluczowe: *reaktory zderzeniowe*, *mieszanie*, *anemometria obrazowa*, *laserowo indukowana fluorescencja*, *modelowanie wielkowirowe*

* M.Sc. Eng. Krzysztof Wojtas, D.Sc. Ph.D. Eng. Łukasz Makowski, Ph.D. Eng. Wojciech Orciuch, Faculty of Chemical and Process Engineering, Warsaw University of Technology.

1. Introduction

Impinging jets are often used in process industry due to possible almost instantaneous mixing of contacting liquids. This happens due to formation of high values of the rate of energy dissipation in impact zone of inlet streams. Each element of the liquid pass through this region without a possibility of bypassing. The region of high energy dissipation is formulated since kinetic energy of inlet streams is being converted into highly turbulent flow caused by collisions and redirections of the flows in a very small space.

In recent years there has been an increase in interests of practical application of this type of reactors in particular in obtaining nanoparticles in pharmaceutical [1–3] and catalytic processes [4]. Therefore investigations of velocity and concentration distribution inside reactors are very important to validate CFD models especially time-dependent models for like large eddy simulations (LES).

2. Experimental system

The reactors used in this study are shown in figure 1. Both reactors are typical T-mixers with two inlet pipes of diameter equal to d = 7 mm and one outlet pipe with diameter D = 11 mm. Two different positions of feeding pipes were applied. In the symmetric T-mixer the inlet streams enter the mixer symmetrically from two sides of the mixer, whereas in the vortex T-mixers the feeding pipes were places tangentially to the outlet pipes.

Local, instantaneous values of fluid velocity and passive tracer concentration were measured using two techniques: particle image velocimetry (PIV) and planar laser induced fluorescence (PLIF). Double-cavity Nd-YAG 532 nm laser with energy equal to 50 mJ per pulse was used. Laser beam was transformed to a collimated planar laser sheet of thickness $\delta \approx 150$ μm. The laser sheet crossed the experimental system vertically through

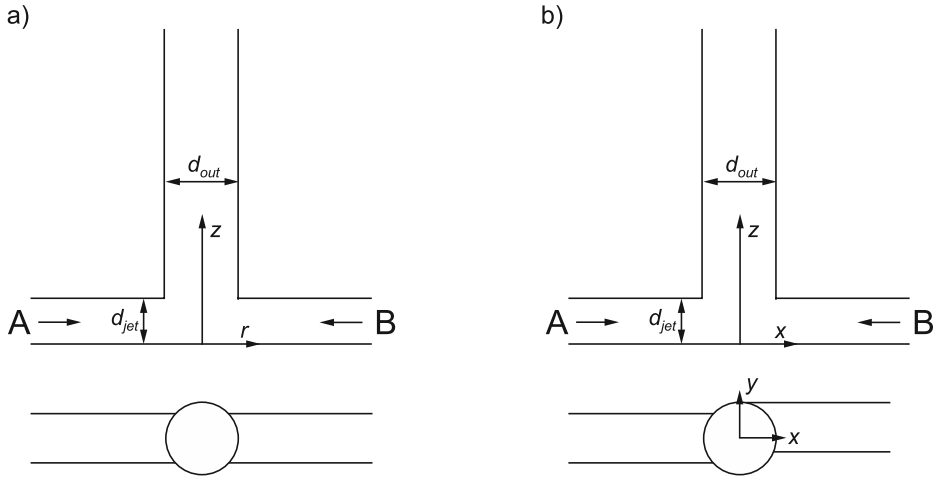


Fig. 1. Geometry of the reactors: a) symmetric T-mixer, b) vortex T-mixer

the axis of the outlet pipe. Polyamide spherical particles of average size equal to 20 μm were used as seeding particles for PIV measurements. The particles were equally dispersed in the inlet solutions and tank inside. Rhodamine B was used as a fluorescent tracer for PLIF measurements and its concentration in the inlet solution c_{in} was equal to 0.2 g m^{-3}. Spatial resolution of PLIF measurements resulted from the resolution of digital images and the thickness of the laser sheet [5]; in our case it was 10 × 10 × 150 μm^3. Spatial resolution of PIV measurements depended also on the size of sampling window and in this work it was 100 × 100 × 150 μm^3. Stream A was double distilled water containing seeding particle. Stream B containing also rhodamine B. Experimentally determined value of local instantaneous mixture fraction f resulted from measured by PLIF local instantaneous value of rhodamine concentration c:

$$f = \frac{c}{c_{in}} \tag{1}$$

3. Simulations

Simulations of hydrodynamics were done using CFD code Ansys Fluent 14. The numerical grid consisted of about 1 800 000 hexahedral computational cells for each reactor. Computations were regarded as satisfactory converged when the total normalized residuals were smaller than 10^{-6}. Two turbulence models were used: the standard k–ε model and large eddy simulation. In LES computations a dynamic stress model was employed to reflect effects of the small scale on large ones.

The distribution of the filtered mean mixture fraction $\bar{f}$ for LES were described using the gradient diffusion approximation. The subgrid diffusivity was based on constant value of the subgrid Schmidt number [6]

$$\frac{\partial \bar{f}}{\partial t} + \bar{u}_i \frac{\partial \bar{f}}{\partial x_i} = \frac{\partial}{\partial x_i}\left[(D_m + D_{\mathrm{SGS}}) \frac{\partial \bar{f}}{\partial x_i} \right] \tag{2}$$

The subgrid concentration variance $\bar{\sigma}'^2$ was predicted by assuming that the small scale statistics can be inferred from the large scale statistic [7]

$$\bar{\sigma}'^2 \approx c_1 \tilde{\sigma}'^2 = c_1 (\tilde{\bar{f}}^2 - \tilde{\bar{f}}^2) \tag{3}$$

where ~ denotes the test-filtered value, computed by applying the test filter (test-filter width 2Δ was used, where Δ is numeric grid size). The constant c_1 is equal to 5 [8]. The mean values of all simulating parameters were obtained using a time-averaging procedure.

The RANS model was completed with the non-equilibrium multiple-time-diffusion model – turbulent mixer model (TMM) [9]. The TMM enables prediction of the distribution of the concentration variance, as well as its inertial-convective, viscous-convective and viscous-diffusive components.

The calculations were performed for Re_{jet} = 250 – 4000, where

$$\mathrm{Re}_{jet} = \frac{u_{jet} d \rho}{\mu} \tag{4}$$

and u_{jet} is mean velocity at the inlet, ρ and μ are density and dynamic viscosity respectively. Values of these parameters were taken as for water at 20°C.

4. Results and discussion

During one measurements 2000 two-dimensional maps of tracer concentration and two components of velocity vector were acquired. The area of the reactor was divided into eight parts which covered completely the whole mixing zone in the reactor. Mean values were calculated from the 2000 instantaneous data. Velocity value was calculated from the values of two components of velocity vector.

Figure 2 and 3 show measured and predicted distributions of mean velocity for Re_{jet} = 1000 and Re_{jet} = 4000. In the case of symmetric T-mixer the Figure 2 shows the results of simulations for *k*–ε and LES models whereas Figure 3 presents only the results for RANS model for vortex T-mixer.

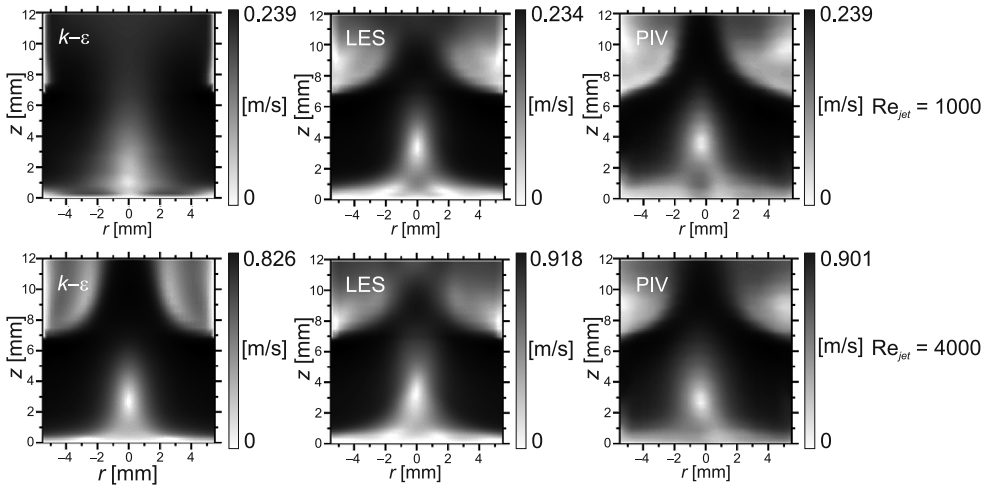


Fig. 2. Distributions of the measured and predicted values of the mean velocity in symmetric T-mixer at the level of injection

The most important region in jet reactors is region of impingement. One can see that agreement between experimental and simulation results in this region is better for large eddy simulation than for the *k*–ε model especially, for lower value of Reynolds number. For high values of Re_{jet} both models predict good results which are in good agreement with experiments, of course it results from theory of the *k*–ε model that was developed for fully

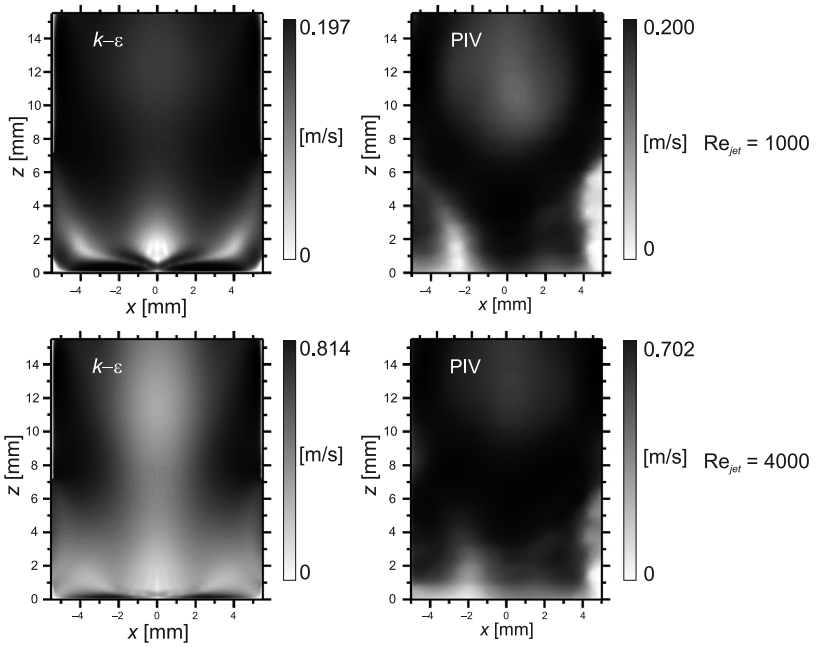


Fig. 3. Distributions of the measured and predicted values of mean velocity in the vortex T-mixer at the level of injection

turbulent flow. The collected data from PLIF experiments, after numerical and statistical analysis, allowed to determine the mixture fraction for two mixed fluids.

The distributions of mean mixture fraction for symmetric T-mixer one can see on the Figure 4. Figure 5 shows examples of instantaneous distribution of mixture fraction. One can clearly see differences between the instantaneous and time averaged values. Figure 6 presents distributions of the mixture fraction variance. Values of the variance for experimental results were calculated from equations:

$$\sigma_s^2 = \int_0^1 [f - \bar{f}]^2 \phi(f)\, df = \frac{1}{N} \sum_{i=1}^{N} [f - \bar{f}]^2 \tag{5}$$

where:

$\phi(f)$ – probability density function,

N – number of two-dimensional maps.

The spatial resolution of the PLIF measurements was close to the size of the smallest scales. Values of RANS calculations overestimated the experimental results whereas the LES results underestimated the experimental results. However one can see that only variance calculating for LES predicted shape of distributions which was similar to the experimental results for presented value of the Reynolds number. The above conclusion applies to the full range of studied Re_{jet}. The results of the large eddy simulation may depend on a model of concentration variance used in computations. Value of the constant c_1 in equation (3) for

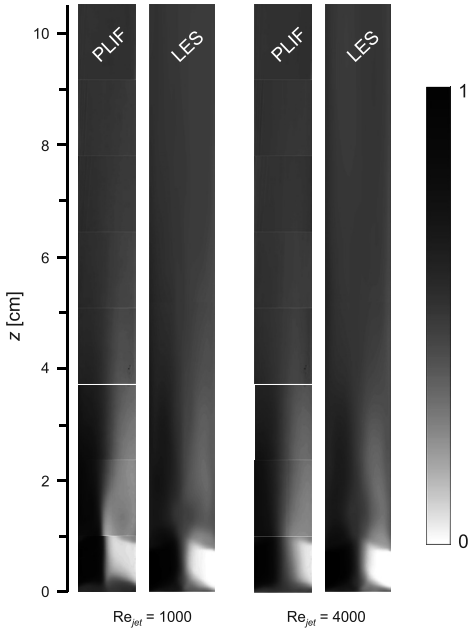


Fig. 4. Distributions of the measured and predicted values of mean mixture fraction in symmetric T-mixer, $Re_{jet} = 1000$

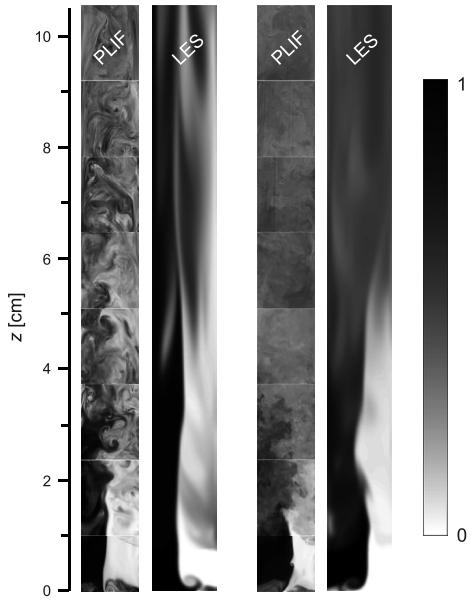


Fig. 5. Distributions of the measured and predicted instantaneous values of the of mixture fraction in symmetric T-mixer for $Re_{jet} = 1000$

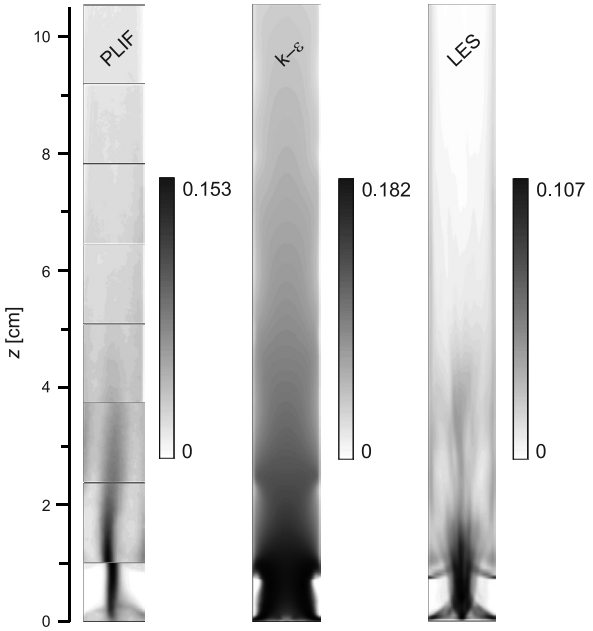


Fig. 6. Distributions of the measured and predicted values of the mixture fraction variance symmetric T-mixer for Re_{jet} = 1000

the high value of the Schmidt number takes c_1 = 5.0 and can be applied after provided the standard LES assumptions for which the numeric scale grid, $\overline{\Delta}$, lies in the inertia-convective subrange. Value of the constant *c* decreases significantly when a scale of numerical grid is of a scale smaller than the Kolmogorov scale. This analysis indicates the need to develop models of concentration variance of passive tracer, especially with dynamic method to determine the model coefficient

5. Conclusions

Instantaneous and mean distributions of velocity and tracer concentration have been measured experimentally by PIV and PLIF techniques and predicted numerically by RANS and LES models. The *k*–ε (RANS) and LES models gave similar results of mean velocity and concentration for high values of the Reynolds number and these results were in good agreement with the experimental data. For lower values of Re_{jet}, like Re_{jet} = 1000, LES results agreed with experimental data much better than the RANS results. Concentration variance has been also determined as an important parameter of fluid segregation decay. In this case the difference between simulation results and experimental data is clearly visible, however the shape of the variance distribution obtained by the LES is well predicted.

Possible improve of LES modelling is to develop new model for concentration variance. Collected experimental data can be used in next works for validation of improved and new LES models of the mixing process.

This work was supported by the by National Science Centre (Decision No DEC-2013/09/B/ST8/02869).

References

[1] Johnson B.K., Prud'homme R.K., *Chemical processing and micromixing in confined impinging jets*, A.I.Ch.E. Journal, vol. 49 , 2003, 2264.
[2] Liu Y., Cheng C., Prud'homme R.K., Fox R.O., *Mixing in a multi-inlet vortex mixer (MIVM) for flash nano-precipitation*, Chem. Engng Sci., vol. 63, 2008, 2829.
[3] Lince F., Marchisio D.L., Barresi A.A., *Strategies to control the particle size distribution of poly-ε-caprolactone nanoparticles for pharmaceutical applications*, Journal of Colloid and Interface Science, vol. 322, 2008, 505.
[4] Marchisio D.L., *Simulation of mixing and reaction in a Confined Impinging Jets reactor*, Comput. Chem. Eng, vol. 33, 2009, 408-420.
[5] Mortensen M., Orciuch W., Bouaifi M., Andersson B., *Mixing of a jet in a pipe*, Chemical Engineering Research and Design, vol. 82, 2004, 357-363.
[6] Jaworski Z., *Numeryczna mechanika płynów w inżynierii chemicznej i procesowej*, Akademicka Oficyna Wydawnicza EXIT, 2005.
[7] Cook A. W., Riley J.J., *A subgrid model for equilibrium chemistry in turbulent flows*, Phys. Fluids, vol. 6, 1994, 2868.
[8] Michioka T., Komori S., *Large-Eddy Simulation of a turbulent reacting liquid flow*, AIChE J., vol. 50, 2004, 2705.
[9] Bałdyga J., *Turbulent mixer model with application to homogenous instantaneous chemical reactions*, Chem. Eng. Sci., vol. 44, 2004, 1175-1182.